Inorg. Chem. **2006**, *45*, 5521–5528

Synthesis, Structural Characterization, Gas Sorption and Guest-Exchange Studies of the Lightweight, Porous Metal–Organic Framework α-$[Mg_3(O_2CH)_6]$

Jeffrey A. Rood, Bruce C. Noll, and Kenneth W. Henderson*

Department of Chemistry and Biochemistry, University of Notre Dame, Notre Dame, Indiana 46556-5670

Received March 30, 2006

Unsolvated magnesium formate crystallizes upon reaction of the metal nitrate with formic acid in DMF at elevated temperatures. Single-crystal XRD studies reveal the formation of $[Mg_3(O_2CH)_6 \supset DMF]$, **1**, a metal–organic framework with DMF molecules filling the channels of an extended diamondoid lattice. The DMF molecules in **1** can be entirely removed without disruption to the framework, giving the guest-free material α-$[Mg_3(O_2CH)_6]$, **2**. Compound **2** has been characterized by both powder and single-crystal XRD studies. Thermogravimetric analyses of **1** show guest loss from 120 to 190 °C, with decomposition of the sample at approximately 417 °C. Gas sorption studies using both N_2 and H_2 indicate that the framework displays permanent porosity. The porosity of the framework is further demonstrated by the ability of **2** to uptake a variety of small molecules upon soaking. Single-crystal XRD studies have been completed on the six inclusion compounds $[Mg_3(O_2CH)_6 \supset THF]$, **3**; $[Mg_3(O_2CH)_6 \supset Et_2O]$, **4**; $[Mg_3(O_2CH)_6 \supset Me_2CO]$, **5**; $[Mg_3(O_2CH)_6 \supset C_6H_6]$, **6**; $[Mg_3(O_2CH)_6 \supset EtOH]$, **7**; and $[Mg_3(O_2CH)_6 \supset MeOH]$, **8**. Analyses of the metrical parameters of **1**–**8** indicate that the framework has the ability to contract or expand depending on the nature of the guest present.

Introduction

Metal−organic frameworks (MOFs) are being studied for use in an ever increasing number of applications[1] including catalysis,[2] optics,[3] electronics,[4] small molecule storage,[5] and separation science.[6] A prerequisite for many of these functions is that the materials display permanent porosity.[7] One of the most popular and successful strategies in the synthesis of porous MOFs has been through the preparation of transition-metal complexes using ditopic organic carboxylate ligands.[8] This is an attractive approach because, in certain instances, the dimensions of the resulting cavities and channels may be controlled by altering the length of the organic linker.[9]

* To whom correspondence should be addressed. E-mail: khenders@nd.edu. Fax: 574 631 6652. Tel: 574 631 8025.

(1) For general reviews on the potential applications of MOFs see: (a) Mueller, U.; Schubert, M.; Teich, F.; Puetter, H.; Schierle-Arndt, K.; Pastre, J. *J. Mater. Chem.* **2006**, *16*, 626. (b) Champness, N. R. *Dalton Trans*. **2006**, *16*, 626. (c) Champness, N. R.; Schröder, M. *Curr. Opin. Solid State Mater*. **1998**, *3*, 419. (d) Janiak, C. *Dalton Trans*. **2003**, 2781. (e) Papaefstathiou, G. S.; MacGillivray, L. R. *Coord. Chem. Rev*. **2003**, *246*, 169. (f) Braga, D. *Chem Commun*. **2003**, 2751. (g) James, S. L. *Chem. Soc. Rev*. **2003**, *32*, 276. (h) Batten, S. R. *Curr. Opin. Solid State Mater*. **2001**, *5*, 107. (i) Zaworotko, M. J. *Chem Commun*. **2001**, 1. (j) Braga, D. *J. Chem. Soc., Dalton Trans*. **2000**, 3705. (k) Zaworotko, M. J. *Angew. Chem., Int. Ed*. **2000**, *39*, 3052.

(2) (a) Wu, C.; Hu, A.; Zhang, L.; Lin, W. *J. Am. Chem. Soc*. **2005**, *127*, 8940. (b) Perles, J.; Iglesias, M.; Martin-Luengo, M.; Monge, M. A.; Ruiz-Valero, C.; Snejko, N. *Chem. Mater*. **2005**, *17*, 5837. (c) Uemara, T.; Kitagawa, K.; Horike, S.; Kawamura, T.; Kitagawa, S. *Chem. Commun*. **2005**, 5968. (d) Schlichte, K.; Kratzke, T.; Kaskel, S. *Microporous Mesoporous Mater*. **2004**, *73*, 81. (e) Seo, J. S.; Whang, D.; Lee, H.; Jun, S. I.; Oh, J.; Jeon, Y.; Kim, K. *Nature* **2000**, *404*, 982. (f) Fujita, M.; Kwon, Y. J.; Washizu, S.; Ogura, K. J. *J. Am. Chem. Soc*. **1994**, *116*, 1151.

(3) (a) Zhang, L.; Yu, J.; Xu, J.; Lu, J.; Bie, H.; Zhang, X. *Inorg. Chem. Commun*. **2005**, *8*, 638. (b) Zhao, B.; Chen, X. Y.; Cheng, P.; Liao, D. Z.; Yan, S. P.; Jiang, Z. H. *J. Am. Chem Soc*. **2004**, *126*, 15394.

(4) (a) Wang, L.; Yang, M.; Shi, Z.; Chen, Y.; Feng, J. *J. Solid State Chem*. **2005**, *178*, 3359. (b) Dietzel, P. D. C.; Morita, Y.; Blom, R.; Fjellvaag, H. *Angew. Chem., Int. Ed*. **2005**, *44*, 6354. (c) Poulsen, R. D.; Bentien, A.; Chevalier, M.; Iversen, B. B. *J. Am. Chem. Soc*. **2005**, *127*, 9156. (d) Cui, H.; Takahashi, K.; Okano, Y.; Kobayashi, H.; Wang, Z.; Kobayashi, A. *Angew. Chem., Int. Ed*. **2005**, *44*, 6508.

(5) (a) Lee, Y. J.; Li, J.; Jagiello, J. *J. Solid State Chem*. **2005**, *178*, 2527. (b) Wang, Q. M.; Shen, D. M.; Bulow, M.; Lau, M. L.; Deng, S. G.; Fitch, F. R.; Lemcoff, N. O.; Semanscin, J. *Microporous Mesoporous Mater*. **2002**, *55*, 217. (c) Fletcher, A. J.; Cussen, E. J.; Prior, T. J.; Rosseinsky, M. J. *J. Am. Chem. Soc*. **2001**, *123*, 10001.

(6) (a) Chen, B.; Liang, C.; Yang, J.; Contreras, D. S.; Clancy, Y. L.; Lobkovsky, E. B.; Yaghi, O. M.; Dai, S. *Angew. Chem., Int. Ed*. **2006**, *45*, 1390. (b) Choi, H. J.; Suh, M. P. *J. Am. Chem. Soc*. **2004**, *126*, 15844. (c) Ohmori, O.; Kawano, M.; Fujita, M. *J. Am. Chem. Soc*. **2004**, *126*, 16292. (c) Dybtsev, D. N.; Chun, H.; Kim, K. *Angew. Chem., Int. Ed*. **2004**, *43*, 5033. (d) Lu, J. Y.; Babb, A. M. *Chem. Commun*. **2002**, 1340.

10.1021/ic060543v CCC: $33.50
Published on Web 06/07/2006

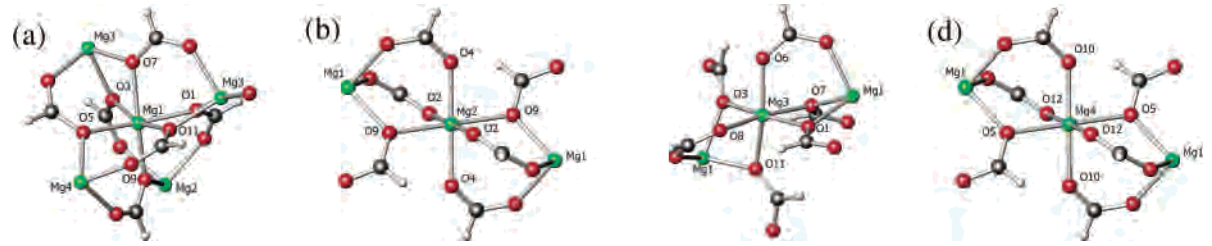

Figure 1. Local geometries surrounding the four independent, octahedrally coordinated magnesium centers within **1**.

The independent studies of Wang,[10] Kim,[11] and Powell[12] have also shown that it is possible to form porous MOFs using even the simplest carboxylate, formate, with a variety of divalent metal ions. Indeed, complete single-crystal X-ray analyses have now been reported for the isomorphous formates of cobalt, α-iron, α-zinc, and β-manganese.[10−12] Gas sorption studies on both the cobalt and the β-manganese formates indicate that they are porous.[10d,11] In addition, similar cell parameters have been determined for α-magnesium formate and nickel formate, although full data collections have not been reported because of handling and sample quality issues.[12a]

Our interests in MOFs have been directed toward the incorporation of *s*-block metals as components of extended networks.[13] Specifically, we have demonstrated that coordination networks may be prepared rationally by linking certain alkali-metal aggregates through neutral ditopic Lewis bases.[14] Constructing MOFs from smaller *s*-block elements is appealing, because they have the potential to form lightweight materials that are attractive candidates for the storage of gases such as dihydrogen and methane.[15,16] Indeed, Long very recently reported that the magnesium dicarboxylate complex $[Mg_3(O_2C-C_{10}H_6-CO_2)_3]$ forms a porous framework that has a relatively high binding affinity for H_2.[17]

We were drawn to the possibility of preparing lightweight, porous MOFs by combining an *s*-block metal with a small carboxylate linker. Herein, we describe the high-temperature synthesis and full structural characterization of magnesium MOF $[Mg_3(O_2CH)_6 \supset DMF]$, **1**. The DMF molecules in **1** can be removed without disrupting the framework. The guest-free material $[Mg_3(O_2CH)_6]$, **2**, was characterized by single-crystal and powder X-ray diffraction (XRD) experiments, as well as by IR and ^1H NMR spectroscopy. Both N_2 and H_2 gas sorption studies on **2** confirmed that the material exhibits permanent porosity. Furthermore, compound **2** uptakes a variety of guest molecules from solution, and single-crystal XRD studies of six new inclusion compounds, $[Mg_3(O_2CH)_6 \supset THF]$, **3**; $[Mg_3(O_2CH)_6 \supset Et_2O]$, **4**; $[Mg_3(O_2CH)_6 \supset Me_2CO]$, **5**; $[Mg_3(O_2CH)_6 \supset C_6H_6]$, **6**; $[Mg_3(O_2CH)_6 \supset EtOH]$, **7**; and $[Mg_3(O_2CH)_6 \supset MeOH]$, **8**, have been completed and will be outlined for comparative purposes. Finally, we also applied our synthetic strategy to prepare the Ca, Sr, and Ba formates, and these studies will be briefly detailed.

Experimental Section

General Procedures. DMF, benzene, acetone, methanol, ethanol, and cyclohexane were dried by distillation over calcium hydride and stored over 4 Å molecular sieves prior to use. THF and Et_2O were purified by passage through a solvent purification system (Innovative Technology). The metal nitrates $Mg(NO_3)_2 \cdot 6H_2O$, $Ca(NO_3)_2 \cdot 4H_2O$, $Sr(NO_3)_2$, $Ba(NO_3)_2$, and formic acid were purchased from Aldrich and used as received. D_2O was purchased from

(7) (a) Dybtsev, D. N.; Nuzdhin, A. L.; Chun, H.; Bryliakov, K. P.; Talsi, E. P.; Fedin, V. P.; Kim, K. *Angew. Chem., Int. Ed.* **2006**, *45*, 916. (b) Wu, C.; Lin, W. *Chem. Commun.* **2005**, 3673. (c) Ma, B.; Mulfort, K. L.; Hupp, J. T. *Inorg. Chem.* **2005**, *44*, 4912. (d) Lee, E. Y.; Jang, S. Y.; Suh, M. P. *J. Am. Chem. Soc.* **2005**, *127*, 6374. (e) Rowsell, J. L. C.; Yaghi O. M. *Microporous Mesoporous Mater.* **2004**, *73*, 3. (f) Rosseinsky, M. J. *Microporous Mesoporous Mater.* **2004**, *73*, 15.

(8) For examples see: (a) Roswell, J. L. C.; Yaghi, O. M. *Angew. Chem., Int. Ed.* **2005**, *44*, 4670. (b) Rosi, N. L.; Kim, J.; Eddaoudi, M.; Chen, B.; O'Keefe, M.; Yaghi, O. M. *J. Am. Chem. Soc.* **2005**, *127*, 1504. (c) Yaghi, O. M.; O'Keefe, M.; Ockwig, N.; Chae, H. K.; Eddaoudi, M.; Kim, J. *Nature* **2003**, *423*, 705. (d) Eddaoudi, M.; Moler, D.; Li, H.; Reinke, T. M.; O'Keefe, M.; Yaghi, O. M. *Acc. Chem. Res.* **2001**, *34*, 319. (e) Kim, J.; Chen, B.; Reinke, T. M.; Li, H.; Eddaoudi, M.; Moler, D. B.; O'Keefe, M.; Yaghi, O. M. *J. Am. Chem. Soc.* **2001**, *123*, 8239. (f) O'Keefe, M.; Eddaoudi, M.; Li, H.; Reinke, T.; Yaghi, O. M. *J. Solid State Chem.* **2000**, *152*, 3. (g) Reinke, T. M.; Eddaoudi, M.; O'Keefe, M.; Yaghi, O. M. *Angew. Chem., Int. Ed.* **1999**, *38*, 2590. (h) Eddaoudi, M.; Li, H.; Reinke, T.; Fehr, M.; Kelley, D.; Groy, T. L.; Yaghi, O. M. *Top. Catal.* **1999**, *9*, 105.

(9) Eddaoudi, M.; Kim, J.; Rosi, N.; Vodak, D.; Wachter, J.; O'Keefe, M.; Yaghi, O. M. *Science* **2002**, *295*, 469.

(10) (a) Wang, Z.; Zhang, B.; Fujiwara, H.; Kobayashi, H.; Kurmoo, M. *Chem. Commun.* **2004**, 416. (b) Wang, Z.; Zhang, B.; Otsuka, T.; Inoue, K.; Kobayashi, H.; Kurmoo, M. *Dalton Trans.* **2004**, 2209. (c) Cui, H.; Takahashi, K.; Okana, Y.; Kobayashi, H.; Wang, Z.; Kobayashi, A. *Angew. Chem. Int. Ed.* **2005**, *44*, 6508. (d) Wang, Z.; Zhang, B.; Kurmoo, M.; Green, M. A.; Fujiwara, H.; Otsuka, T.; Kobayashi, H. *Inorg. Chem.* **2005**, *44*, 1230.

(11) Dybstev, D. N.; Chun, H.; Yoon, S. H.; Kim, D.; Kim, K. *J. Am. Chem. Soc.*, **2004**, *126*, 32.

(12) (a) Viertelhaus, M.; Adler, P.; Clerac, R.; Anson, C. E.; Powell, A. K. *Eur. J. Inorg. Chem.* **2005**, *4*, 692. (b) Viertelhaus, M.; Anson, C. E.; Powell, A. K. *Z. Anorg. Allg. Chem.* **2005**, *631*, 2365. (c) Viertelhaus, M.; Henke, H.; Anson, C. E.; Powell, A. K. *Eur. J. Inorg. Chem.* **2003**, *12*, 2283.

(13) For examples of networks incorporating *s*-block metals see: (a) Son, S. U.; Reingold, J. A.; Kim, S. B.; Carpenter, G. B.; Sweigart, D. A. *Angew. Chem., Int. Ed.* **2005**, *44*, 7710. (b) de Lill, D. T.; Bozzuto, D. J.; Cahill, C. L. *Dalton Trans.* **2005**, 2111. (c) Kennedy, A. R.; Kirkhouse, J. B. A.; McCarney, K. M.; Puissegur, O.; Smith, W. E.; Staunton, E.; Teat, S. J.; Cherryman, J. C.; James, R. *Chem.—Eur. J.* **2004**, *10*, 4606. (d) Côte, A. P.; Shimizu, K. W. *Chem.—Eur. J.* **2003**, *9*, 5361. (e) Richards, P. I.; Benson, M. A.; Steiner, A. *Chem. Commun.* **2003**, 1392.

(14) (a) Morris, J. J.; Noll, B. C.; Henderson, K. W. *Cryst. Growth Des.* **2006**, *6*, 1071. (b) MacDougall, D. J.; Morris, J. J.; Noll, B. C.; Henderson, K. W. *Chem. Commun.* **2005**, 456. (c) MacDougall, D. J.; Noll, B. C.; Henderson, K. W. *Inorg. Chem.* **2005**, *44*, 1181. (d) Henderson, K. W.; Kennedy, A. R.; MacDougall, D. J. *Phosphorous, Sulfur Silicon Relat. Elem.* **2004**, *179*, 795. (e) Henderson, K. W.; Kennedy, A. R.; Macdonald, L.; MacDougall, D. J. *Inorg. Chem.* **2003**, *42*, 2839. (f) Henderson, K. W.; Kennedy, A. R.; McKeown, A. E.; Strachan, D. *J. Chem. Soc., Dalton Trans.* **2000**, 4348.

(15) (a) Rowsell, J. L. C.; Yaghi, O. M. *J. Am. Chem. Soc.* **2006**, *128*, 1304. (b) Chen, B.; Ockwig, N. W.; Millward, A. R.; Contreras, D. S.; Yaghi, O. M. *Angew. Chem., Int. Ed.* **2005**, *44*, 4745. (c) Rowsell, J. L. C.; Eckert, J.; Yaghi, O. M. *J. Am. Chem. Soc.* **2005**, *127*, 14904.

(16) Schlapbach, L.; Züttel, A. *Nature* **2001**, *414*, 353.

(17) Dincă, M.; Long, J. R. *J. Am. Chem. Soc.* **2005**, *127*, 9376.

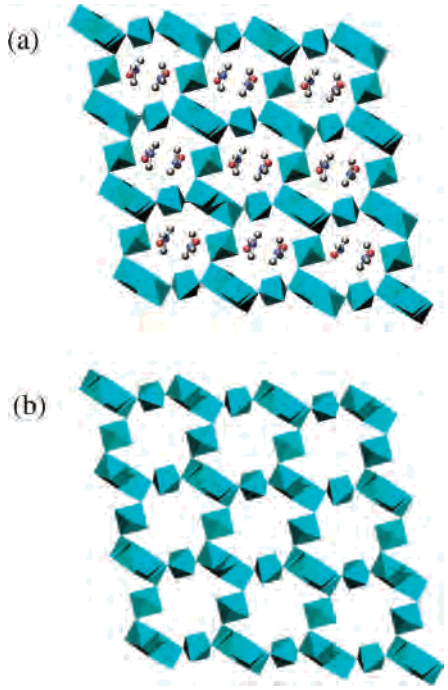

Figure 2. (a) View of the extended structure of **1** down the crystallographic *b* axis showing DMF molecules within the channels. (b) A similar view of **2**, illustrating that the integrity of the framework is retained upon guest removal. For clarity, the frameworks are depicted as interconnected MgO_6 octahedral units.

Cambridge Isotope Laboratories and was used for the ^{1}H NMR spectroscopic studies. ^{1}H NMR spectra were recorded on a Varian-300 spectrometer at 293 K and were referenced internally to the residual signals of the deuterated solvent. FTIR spectra were obtained as Nujol mulls on a Perkin−Elmer Paragon 1000 FTIR spectrometer in the range of 4000−650 cm^{-1}. Thermogravimetric analyses were performed on a TA instruments hi-res modulated TGA 2950 thermogravimetric analyzer at a rate of 10 °C/min under N_2. Elemental analyses were performed by Midwest Microlab, Indianapolis, IN. The N_2 and H_2 sorption experiments were carried out at 77.4 K at Quantachrome Instruments, Boynton Beach, FL.

Synthesis of [$Mg_3(O_2CH)_6$⊃DMF], 1. A mixture of 10 mL DMF, 0.23 mL of formic acid (6 mmol), and 0.77 g of $Mg(NO_3)_2$·$6H_2O$ (3 mmol) was placed in a 20 mL scintillation vial. The vial was capped and immersed in a silicon oil bath that was kept at a constant temperature of 110 °C for 40 h. During this period, high-quality crystals of **1** were deposited (0.34 g, 81.7%). The crystals could then be filtered in air until dry. Anal. Calcd for **1**, $C_9H_{13}O_{13}NMg_3$: C, 25.97; H, 3.15; N, 3.36. Found: C, 24.55; H, 3.66; N, 3.01. IR bands (cm^{-1}) for **1** (Nujol mull): 3306 m, 2924 s, 2854 s, 1670 s, 1608 s, 1460 m, 1417 m, 1396 s, 1376 m, 1350 s, 1259 w, 1099 w, 790 w, 722 w, 662 w. ^{1}H NMR (D_2O): δ 2.84 $N(CH_3)_2$, 3.00 $N(CH_3)_2$, 7.92 OCH, 8.44 O_2CH. TGA studies on **1** are outlined in Figure 3. Results from the N_2 and H_2 gas sorption studies are shown in Figures 5 and 6, respectively.

Synthesis of [$Mg_3(O_2CH)_6$], 2. A sample of **1** was evacuated using a two-stage rotary pump and heated to 130 °C for 36 h. The crystals were subsequently used for single-crystal and powder XRD studies. Powder XRD studies are outlined in Figure 4 and areconsistent with retention of the framework upon evacuation. IR bands (cm^{-1}) for **2** (Nujol mull): 3300 m, 2924 s, 2854 s, 1674 m, 1636 s, 1610 s, 1460 m, 1415 w, 1405 w, 1376 m, 1347 s, 790 w, 722 w. ^{1}H NMR (D_2O): δ 8.44 O_2CH.

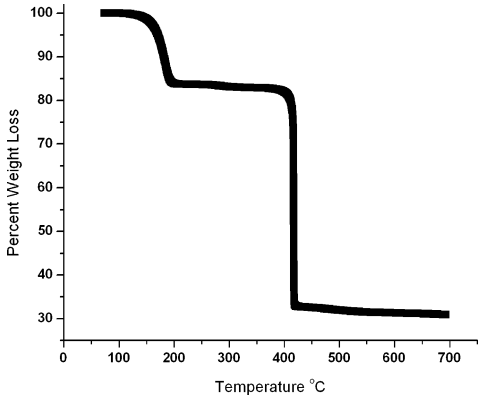

Figure 3. Thermogravimetric analysis of **1** (10 °C/min under N_2).

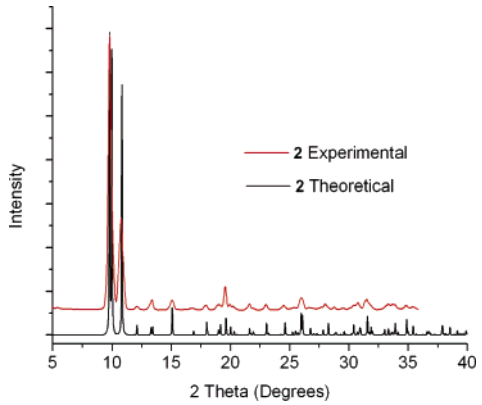

Figure 4. Theoretical powder XRD pattern based on the structure of **2** (black) at 100 K and the observed pattern for **2** at ambient temperature (red).

Syntheses of *β*-[$Ca(O_2CH)_2$], 13; α-[$Sr(O_2CH)_2$], 14; and [$Ba_3(O_2CH)_{5.67}(NO_3)_{0.33}$], 15. The attempted syntheses of the calcium, strontium, and barium formates were carried out in a manner similar to that outlined above for **1**. The calcium and strontium reactions resulted in the preparation of the known, nonporous phases *β*-[$Ca(O_2CH)_2$] and α-[$Sr(O_2CH)_2$]. Full data collections and solution refinements were carried out by single-crystal XRD on the samples at 100 K, as low-temperature analyses of these compounds have not previously been reported. Crystallographic data for **13** and **14** are supplied in the Supporting Information in CIF format. Repeated reactions involving barium nitrate resulted in the deposition of small amounts of crystals along with large quantities of powder. Single-crystal XRD studies revealed a unique unit cell, and the extended structure was found to be very similar to that of barium formate but with a single disordered ligand site. The best-fit model for this site suggested partial occupancy of nitrate for formate to give a formula of [$Ba_3(O_2CH)_{5.67}(NO_3)_{0.33}$]. We were unable to prepare compound **15** as a single-phase species, which made further characterization problematic. Crystallographic data for **15** are supplied in the Supporting Information in CIF format.

Guest-Inclusion Studies. Eight solvent systems were studied for their guest-inclusion behavior: DMF, THF, Et_2O, acetone, benzene, ethanol, methanol and cyclohexane. Crystalline samples of **2** were soaked in 2 mL of neat solvent, or mixtures of solvents for the selectivity studies, inside a capped vial. The mixtures were allowed to stand for 48 h, after which time the crystals were filtered in air until dry. The samples were then analyzed by single-crystal XRD and ^{1}H NMR spectroscopy. With the exception of cyclohexane, all of the solvents were found to diffuse into the framework to give the seven inclusion compounds: [$Mg_3(O_2CH)_6$⊃DMF], **1**;

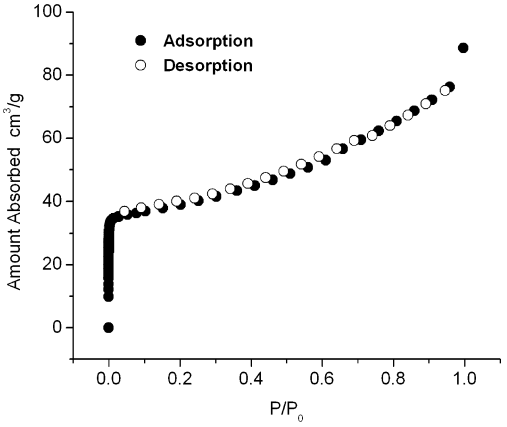

Figure 5. BET N_2 isotherm for **1** at 77.4 K.

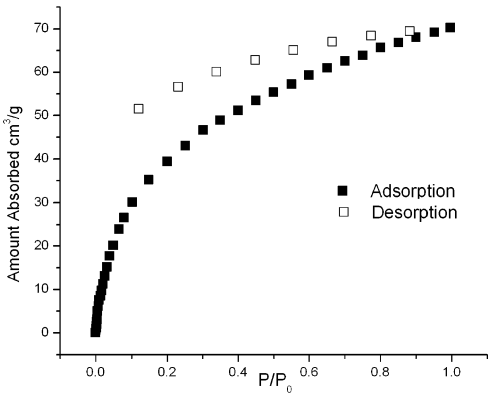

Figure 6. BET H_2 sorption isotherm for **1** at 77.4 K.

$[Mg_3(O_2CH)_6 \supset THF]$, **3**; $[Mg_3(O_2CH)_6 \supset Et_2O]$, **4**; $[Mg_3(O_2CH)_6 \supset Me_2CO]$, **5**; $[Mg_3(O_2CH)_6 \supset C_6H_6]$, **6**; $[Mg_3(O_2CH)_6 \supset EtOH]$, **7**, and $[Mg_3(O_2CH)_6 \supset MeOH]$, **8**.

X-ray Crystallography. Powder XRD patterns were obtained on a Bruker Smart Apex diffractometer with Cu Kα radiation. The sample was mounted in a capillary. Data were collected by the 2D Apex detector fixed at 100 mm, 20° 2θ, 0° ω, 0° ϕ for 10 min.

Single crystals were examined under Infineum V8512 oil. The datum crystal was affixed to either a thin glass fiber atop a tapered copper mounting pin or Mitegen mounting loop and transferred to the 100 K nitrogen stream of a Bruker APEX diffractometer equipped with an Oxford Cryosystems 700 series low-temperature apparatus. Cell parameters were determined using reflections harvested from three sets of 12 0.5° ϕ scans. The orientation matrix derived from this was transferred to COSMO[18] to determine the optimum data collection strategy that required a minimum 4-fold redundancy. Cell parameters were refined using reflections harvested from the data collection with $I \geq 10\sigma(I)$. All data were corrected for Lorentz and polarization effects, and runs were scaled using SADABS.[19]

The structures were solved from partial data sets using the Autostructure option in APEX 2.[18] This option employs an iterative application of the direct methods, Patterson synthesis, and dual-space routines of SHELXTL.[20] Hydrogen atoms were placed at calculated geometries and allowed to ride on the position of the parent atom. Hydrogen thermal parameters were set to 1.2× the equivalent isotropic U of the parent atom.

(18) *APEX2* and *COSMO*; Bruker−Nonius AXS: Madison, WI, 2005.
(19) Sheldrick, G. M. *SADABS*; Bruker−Nonius AXS: Madison, WI, 2004.
(20) Sheldrick, G. M. *SHELXTL*; Bruker−Nonius AXS: Madison, WI, 2004.

Results and Discussion

Syntheses and Structural Characterizations. To place the present work in context, we first discuss the previously characterized compounds of magnesium formate. Two different crystalline forms of magnesium formate dihydrate, $[Mg(O_2CH)_2 \cdot 2H_2O]$, α-**9** and β-**9**, have been structurally characterized.[21,22] One form, α-**9**, is monoclinic with space group $P2_1/c$. The structure is composed of two independent magnesium centers, where one metal is surrounded by six different formate groups and the second metal is surrounded by two formates and four water molecules. These octahedral centers then interconnect to form a three-dimensional network. In contrast, β-**9** crystallizes in the orthorhombic space group *Pbca*. This structure contains a single type of magnesium, which is octahedrally coordinated but in this instance connects to two axial water molecules and four equatorial formates. The formates then bridge to neighboring metal centers to form a two-dimensional (4,4) square net arrangement.[23] Compound α-**9** has been prepared by a variety of means, including the reaction of Mg powder,[22] MgO,[24] $MgCO_3$,[25] or $Mg(OEt)_2$[26] with excess formic acid, followed by recrystallization. The transmetalation of sodium, potassium, or ammonium formate with either $MgCl_2$ or $Mg(NO_3)_2$ has also successfully been applied for the synthesis of α-**9**.[22] Compound β-**9** is reported to be prepared as a minor product during the synthesis of α-**9** and could not be obtained as a single phase material.[22]

A two-dimensional sheet structure similar to that of β-**9** is found for complex $[Mg(O_2CH)_2 \cdot 2(NH_2)_2CO]$, **10**.[27] Again, the metals are octahedrally coordinated in **10**, with four bridging equatorial formate groups but now with two terminal urea units. This material was crystallized from a concentrated aqueous solution of the complex, which was maintained at 45 °C for several weeks.

Powell recently disclosed that at least two forms, α and β, of unsolvated magnesium formate may be prepared using solvothermal conditions.[12] Specifically, heating a mixture of $[Mg(O_2CH)_2 \cdot 2H_2O]$ in formic acid at 120 °C for several days in a sealed steel autoclave fitted with a Teflon sleeve resulted in the preparation of $[Mg_3(O_2CH)_6 \supset HCO_2H]$, **11**, i.e., the α form of the salt. The same group went on to show that increasing the reaction temperature to 170 °C yielded the nonporous formate β-$[Mg(O_2CH)_2]$, **12**. As mentioned in the Introduction, complex **11** was not fully characterized because of the formation of only microcrystalline material. Nevertheless, the structure and composition of **11** was inferred through comparison of its unit cell parameters with related metal

(21) Osaki, K.; Nakai, Y.; Watanabe, T. *J. Phys. Soc. Jpn.* **1963**, *18*, 919.
(22) Melard, C.; Pezerat, H.; Herpin, P.; Toledano, P. *J. Solid State Chem.* **1982**, *41*, 67.
(23) Wells, A. F. *Three-Dimensional Nets and Polyhedra*; Wiley-Interscience: New York, 1977.
(24) Dollimore, D.; Gupta, J. P.; Nowell, D. V. *Thermochim. Acta* **1979**, *30*, 339.
(25) DeWith, G.; Harkema, S.; VanHummel, G. J. *Acta Crystallogr., Sect. B* **1976**, *32*, 1980.
(26) Coker, E. N.; Boyle, T. J.; Rodriguez, M. A.; Alam, T. A. *Polyhedron* **2004**, *23*, 1739.
(27) Yamagata, K.; Achiwa, N.; Hashimoto, M.; Koyano, N.; Ridwan, Y. I.; Shibuya, I. *Acta Crystallogr., Sect. C* **1992**, *48*, 793.

Table 1. Crystallographic Data for Compounds **1**−**8**

	1	**2**	**3**	**4**
formula	$C_9H_{13}Mg_3NO_{13}$	$C_6H_6Mg_3O_{12}$	$C_{10}H_{14}Mg_3O_{13}$	$C_8H_{11}Mg_3O_{12.5}$
fw	416.13	343.022	415.129	380.10
T (K)	100(2)	100(2)	100(2)	100(2)
cryst syst	monoclinic	monoclinic	monoclinic	monoclinic
space group	$P2_1/n$	$P2_1/n$	$P2_1/n$	$P2_1/n$
a (Å)	11.4007(6)	11.324(2)	11.307(18)	11.380(4)
b (Å)	9.9047(4)	9.847(2)	9.857(16)	9.841(3)
c (Å(	14.5357(6)	14.623(3)	14.729(3)	14.506(5)
α (deg)	90	90	90	90
β (deg)	91.317(2)	91.150(3)	91.371(3)	91.429(2)
γ (deg)	90	90	90	90
V (Å^3)	1640.94(13)	1630.2(6)	1641.1(5)	1624.00(9)
Z	4	4	4	4
D (Mg/m^3)	1.684	1.398	1.680	1.797
μ (Mo Kα) (mm^{-1})	0.256	0.235	0.254	0.246
cryst size (mm^3)	0.38 × 0.35 × 0.29	0.30 × 0.23 × 0.20	0.26 × 0.22 × 0.19	0.28 × 0.22 × 0.20
T_{max}, T_{min}	0.94, 0.91	0.96, 0.94	0.96, 0.93	0.96, 0.94
θ range (deg)	2.25−33.19	5.55−30.50	2.24−31.52	2.25−34.40
no. of reflns collected	33 828	14 160	28 698	49 875
no. of ind reflns	5725	4911	6383	5911
R(int)	0.0353	0.0230	0.0263	0.020
no. of obs. reflns [$I > 2\sigma(I)$]	4746	4142	5836	2241
R1[a], wR2[b] [$I > 2\sigma(I)$]	0.0302, 0.0754	0.0260, 0.0642	0.0320, 0.0970	0.0468, 0.1294
R1[a], wR2[b] (all data)	0.0400, 0.0791	0.0341, 0.0679	0.0359, 0.1020	0.0628, 0.1363
GOF[c] on F^2	1.047	1.058	1.179	1.633
largest peak/hole (e Å^{-3})	0.308 and −0.383	0.399 and −0.225	0.427 and −0.668	0.631 and −0.572

	5	**6**	**7**	**8**
formula	$C_9H_{12}Mg_3O_{13}$	$C_{12}H_{12}Mg_3O_{12}$	$C_8H_{12}Mg_3O_{13}$	$C_7H_{10}Mg_3O_{13}$
fw	401.12	421.5	389.11	375.08
T (K)	100(2)	100(2)	100(2)	100(2)
cryst syst	monoclinic	monoclinic	monoclinic	monoclinic
space group	$P2_1/n$	$P2_1/n$	$P2_1/n$	$P2_1/n$
a (Å)	11.2790(8)	11.3762(10)	11.296(3)	11.289(7)
b (Å)	9.8339(7)	9.9831(9)	9.818(3)	9.818(6)
c (Å(	14.7660(11)	15.0358(13)	14.585(4)	14.546(7)
α (deg)	90	90	90	90
β (deg)	91.565(4)	91. 203(5)	91.662(10)	91.622(3)
γ (deg)	90	90	90	90
V (Å^3)	1637.2(2)	1707.2(3)	1616.92(8	1611.6(18)
Z	4	4	4	4
D (Mg/m^3)	1.627	1.639	1.598	1.546
μ (Mo Kα) (mm^{-1})	0.251	0.241	0.252	0.249
cryst size (mm^3)	0.3 × 0.25 × 0.22	0.32 × 0.25 × 0.22	0.15 × 0.13 × 0.13	0.31 × 0.23 × 0.22
T_{max}, T_{min}	0.95, 0.92	0.95, 0.93	0.97, 0.96	0.95, 0.93
θ range (deg)	2.24−31.64	2.22−31.60	2.25−27.55	2.25−25.08
no. of reflns collected	41 801	26 694	39 296	10 078
no. of ind reflns	5480	19456	3724	2859
R(int)	0.0331	0.036	0.0294	0.0513
no. of obs. reflns [$I > 2\sigma(I)$]	4750	4477	3476	2507
R1[a], wR2[b] [$I > 2\sigma(I)$]	0.0433, 0.1173	0.0477, 0.0919	0.0411, 0.1033	0.0407, 0.1230
R1[a], wR2[b] (all data)	0.0510, 0.1213	0.0348, 0.0825	0.0444, 0.1044	0.0469, 0.1270
GOF[c] on F^2	1.154	1.043	1.295	1.129
largest peak/hole (e Å^{-3})	0.875 and −0.679	0.606 and − 0.679	0.426 and −0.668	0.909 and −0.331

[a] $R1 = \sum||F_o| - |F_c||/\sum|F_o|$. [b] $wR2 = \{\sum[w(F_o^2 - F_c^2)^2]/\sum[w(F_o^2)^2]\}^{1/2}$; $w^{-1} = [\sigma^2(F_o^2) + (0.1325P)^2 + 9.6648P]$; $P = (F_o^2 + 2F_c^2)/3$. [c] $GOF = S = \{\sum[w(F_o^2 - F_c^2)^2]/(n - p)\}^{1/2}$; n= number of reflections; p =number of parameters.

formate complexes and by IR spectroscopic studies and weight loss experiments. No such problems were encountered for **12**, which was found to adopt a three-dimensional structure composed of interconnecting chains of fused MgO_6 octahedra.[12b]

We opted to investigate the high-temperature synthesis of magnesium formate from the reaction of magnesium nitrate with formic acid, using DMF as solvent media. Variations on this method have been successfully applied to the synthesis of a number of MOFs, including β-manganese formate.[11] It was hoped that employing milder synthetic conditions compared to the solvothermal conditions previously used would aid in the preparation of high-quality crystals of the potentially porous α-form of magnesium formate. This approach proved successful by maintaining the reaction mixture at approximately 110 °C for several days, producing a large batch of excellent-quality single crystals (see the Experimental Section). Subsequent XRD analysis of the crystals confirmed that the framework of [$Mg_3(O_2CH)_6$⊃DMF], **1**, is isomorphous with that of the previously characterized cobalt, α-iron, α-zinc, and β-manganese formates and is essentially in accord with the reported cell parameters of compound **11** (Table 1).[10−12] As shown in Figure 1, the solid-state structure of **1** contains four crys-

Table 2. Comparison of Mg−O Bond Distances (Å) for **1**−**8**[a]

	weighted average[b]	range	Δ
Mg(1)−O(1)	2.0815(12)	2.0867−2.0758	0.0109
Mg(1)−O(3)	2.0986(13)	2.1023−2.0929	0.0094
Mg(1)−O(5)	2.0763(12)	2.0821−2.0709	0.0112
Mg(1)−O(7)	2.1031(12)	2.1227−2.089	0.0337
Mg(1)−O(9)	2.0624(12)	2.0671−2.053	0.0141
Mg(1)−O(11)	2.0904(12)	2.1002−2.0834	0.0168
Mg(2)−O(2)	2.0561(12)	2.0641−2.0508	0.0133
Mg(2)−O(4)	2.0500(12)	2.0552−2.042	0.0132
Mg(2)−O(9)	2.1193(11)	2.1264−2.1118	0.0146
Mg(3)−O(1)$^{\#3}$	2.0641(13)	2.0684−2.0533	0.0151
Mg(3)−O(3)	2.0833(13)	2.09−2.0734	0.0166
Mg(3)−O(6)	2.0271(13)	2.0339−2.0199	0.0140
Mg(3)−O(7)	2.0910(12)	2.0982−2.0804	0.0178
Mg(3)−O(8)	2.0275(13)	2.0342−2.0216	0.0126
Mg(3)−O(11)$^{\#3}$	2.1094(13)	2.1143−2.0974	0.0169
Mg(4)−O(5)	2.1112(11)	2.1186−2.1056	0.0130
Mg(4)−O(10)	2.0365(12)	2.0458−2.0273	0.0185
Mg(4)−O(12)	2.0529(12)	2.0628−2.0443	0.0185

[a] Symmetry transformations used to generate equivalent atoms: #3 $-x + {}^1/_2, y - {}^1/_2, -z + {}^3/_2$. [b] Formula for weighted average: $x_{\mathrm{wax}} = \sum w_i x_i / \sum w_i$; $w_i = 1/\sigma_i^2$. Formula for standard deviation: $\sigma = \sqrt{\sum \sigma_i^2 / N}$

tallographically independent metal centers, each of which are octahedrally coordinated by six different formate anions. All of the formates adopt similar binding modes, with one oxygen connecting to a single metal center and the second oxygen bridging between two other metals. This η^2, μ^3 bonding motif of the formate anions is also seen in β-[Mg(O$_2$CH)$_2$], **12**,[12b] but differs from the simple η^2, μ^2 bridging mode found for the other structurally characterized formates of magnesium. The C−O distances in **1** lie in the narrow range 1.2325(12)−1.2843(11) Å and are consistent with delocalized bonding within carboxylate backbones.[28]

Although each formate adopts a similar bonding mode, there are three different coordination environments for the metal centers present in **1**. Specifically, Mg(1) bonds to six μ^2-oxygens; Mg(2) and Mg(4) each bond to four μ^1-oxygens and two μ^2-oxygens, whereas Mg(3) bonds to two μ^1-oxygens and four μ^2-oxygens. The extended structure may be viewed as one-dimensional chains of edge-shared MgO$_6$ octahedra, Mg(1) and Mg(3), that are linked together by vertex-sharing octahedra, Mg(2) and Mg(4), to create a three-dimensional assembly. Four edge-shared chains connect through vertex-linking octahedra to form channels that run parallel to the crystallographic *b* axis (Figure 2a). In **1**, these channels are occupied by DMF molecules, with one guest per asymmetric unit to give the formula [Mg$_3$(O$_2$CH)$_6$⊃DMF]. The encapsulated guest molecules are not disordered, which is somewhat unusual for a MOF. The windows of the channels are approximately 4.5 Å × 5.5 Å wide, on the basis of the van der Waals radii of the surface atoms. Also, the calculated void space within **1** after excluding the guest DMF molecules is estimated to be 30.9% using PLATON. [29]

Table 3 lists the independent Mg−O bond lengths, and complete listings of the independent Mg−O bond lengths and the O−Mg−O angles within **1** can be found in the Supporting Information. The Mg−O distances range between 2.0283(8) and 2.1304(7) Å, with a mean value of 2.075 Å. The isomorphous frameworks of α-[Fe$_3$(O$_2$CH)$_6$⊃HCO$_2$H], [Co$_3$(O$_2$CH)$_6$⊃(HCO$_2$H)(H$_2$O)], and α−[Zn$_3$(O$_2$CH)$_6$⊃HCO$_2$H] formate have similar M−O ranges of 2.069(4)−2.175(4), 2.042(3)−2.123(3), and 2.023(3)−2.164(2) Å, respectively,[12a] whereas β-[Mn$_3$(O$_2$CH)$_6$⊃(CH$_3$OH)(H$_2$O)] has somewhat longer Mn−O distances in the range 2.116(2)−2.225(2) Å,[10d] in accord with the radii of the metal centers involved.

We also applied the same synthetic method using the heavier alkaline earth metals calcium, strontium, and barium. In each case, the metal nitrates were mixed with formic acid in DMF and allowed to react at temperatures between 90 and 110 °C. The reactions involving calcium and strontium resulted in the preparation of known phases β-[Ca(O$_2$CH)$_2$], **13**, and α-[Sr(O$_2$CH)$_2$], **14**.[30,31] Both calcium and strontium

Table 3. Comparison of O−Mg−O Bond Angles (deg) for **1**−**8**[a]

	weighted average[b]	range	Δ		weighted average	range	Δ
O(9)−Mg(1)−O(5)	95.04(5)	96.24−93.73	2.51	O(6)−Mg(3)−O(3)	90.11(5)	91.01−89.07	1.94
O(5)−Mg(1)−O(1)	170.87(5)	172.08−169.67	2.41	O(8)−Mg(3)−O(11)$^{\#3}$	88.56(5)	89.60−87.67	1.93
O(5)−Mg(1)−O(11)	94.32(5)	95.08−93.23	1.85	O(3)−Mg(3)−O(11)$^{\#3}$	101.20(5)	101.73−100.20	1.53
O(9)−Mg(1)−O(3)	94.78(5)	95.65−94.42	1.23	O(6)−Mg(3)−O(7)	90.45(5)	91.31−89.29	2.02
O(1)−Mg(1)−O(3)	93.62(5)	94.84−93.01	1.83	O(3)−Mg(3)−O(7)	78.33(5)	78.72−78.01	0.71
O(9)−Mg(1)−O(7)	171.51(5)	172.97−171.15	1.82	O(8)−Mg(3)−O(1)$^{\#3}$	94.54(5)	95.10−93.21	1.89
O(1)−Mg(1)−O(7)	87.07(5)	87.83−86.64	1.19	O(8)−Mg(3)−O(3)	93.66(5)	95.07−91.93	3.14
O(3)−Mg(1)−O(7)	77.70(5)	78.15−76.90	1.25	O(1)$^{\#3}$−Mg(3)−O(3)	171.61(5)	172.67−170.87	1.80
O(9)−Mg(1)−O(1)	89.77(5)	91.32−89.09	2.23	O(6)−Mg(3)−O(11)$^{\#3}$	168.13(6)	170.13−167.45	2.68
O(9)−Mg(1)−O(11)	98.60(5)	99.2−97.37	1.83	O(8)−Mg(3)−O(7)	170.48(6)	171.75−169.52	2.23
O(1)−Mg(1)−O(11)	77.31(5)	77.71−77.62	0.09	O(1)$^{\#3}$−Mg(3)−O(7)	93.39(5)	94.85−92.65	2.20
O(5)−Mg(1)−O(3)	93.65(5)	95.6−92.77	2.83	O(11)$^{\#3}$−Mg(3)−O(7)	88.33(5)	89.95−87.56	2.39
O(11)−Mg(1)−O(3)	163.74(5)	164.18−163.71	0.47	O(11)$^{\#3}$−Mg(3)−O(1)	77.67(3)	78.12−77.31	0.81
O(5)−Mg(1)−O(7)	89.18(5)	89.87−88.50	1.37	O(12)−Mg(4)−O(10)	89.39(5)	91.02−88.52	2.50
O(11)−Mg(1)−O(7)	88.32(5)	89.11−87.91	1.20	O(12)$^{\#4}$−Mg(4)−O(5)	87.89(5)	88.39−87.65	0.74
O(4)$^{\#2}$−Mg(2)−O(2)	89.65(5)	90.86−88.32	2.54	O(10)−Mg(4)−O(5)	90.36(5)	91.26−89.93	1.33
O(4)$^{\#2}$−Mg(2)−O(9)	89.72(5)	90.92−88.82	2.10	O(10)−Mg(4)−O(5)$^{\#4}$	89.64(5)	90.16−88.74	1.42
O(4)−Mg(2)−O(2)	90.39(5)	91.68−89.14	2.54	O(12)−Mg(4)−O(10)$^{\#4}$	90.56(5)	91.02−88.98	2.04
O(2)−Mg(2)−O(9)	93.12(5)	93.65−92.27	1.38	O(12)−Mg(4)−O(5)	91.37(5)	92.35−88.06	4.29
O(2)$^{\#2}$−Mg(2)−O(9)	86.88(5)	87.73−86.35	1.38	O(10)$^{\#4}$−Mg(4)−O(5)	89.74(4)	90.16−88.74	1.42
O(8)−Mg(3)−O(6)	94.38(5)	94.83−93.22	1.61	O(12)−Mg(4)−O(5)$^{\#4}$	87.90(5)	88.39−87.65	0.74
O(6)−Mg(3)−O(1)$^{\#3}$	90.11(5)	92.43−89.77	2.66				

[a] Symmetry transformations used to generate equivalent atoms: #2 $-x + 1, -y + 2, -z + 2$; #3 $-x + {}^1/_2, y - {}^1/_2, -z + {}^3/_2$; #4 $-x, -y + 2, -z + 2$. [b] Formula for weighted average: $x_{\mathrm{wav}} = \sum w_i x_i / \sum w_i$; $w_i = 1/\sigma_i^2$. Formula for standard deviation: $\sigma = \sqrt{\sum \sigma_i^2 / N}$.

formate are known to adopt at least four different structural modifications (α, β, γ, and δ).[32] Compounds **13** and **14** are nonporous and do not contain coordinated or encapsulated DMF within their structures. Previous crystallographic studies of **13** and **14** have been conducted at ambient temperatures, and therefore full data sets were collected on these samples at low-temperature (100 K); the data are supplied as Supporting Information but will not be discussed further here.

In comparison, the reactions involving barium consistently deposited small quantities of crystals along with larger amounts of powder. The crystals were found to have different unit cell parameters (orthorhombic, *Pnma*) compared to those of the single known phase of barium formate (orthorhombic, $P2_12_12_1$).[31] Single-crystal XRD revealed a structure that is very closely related to barium formate, but with the distinction of having a partially occupied nitrate site to give a molecular formula of $[Ba_3(O_2CH)_{5.67}(NO_3)_{0.33}]$, **15**. Repeated cell checks of different batches of crystals confirmed the reproducibility of the preparation of **15**. Again, compound **15** is nonporous; details of its structure are available in the Supporting Information but will not be discussed further here.

Thermal Stability, Gas Sorption, and Guest-Exchange Studies. Thermogravimetric analytical studies were conducted on **1** between 73 and 700 °C, and the results are summarized in Figure 3. An initial weight loss from the sample occurred between 120 and 190 °C, followed by a second decomposition at approximately 417 °C. The first weight loss of 16.3% is in reasonable agreement with the calculated value of 17.5% expected by the complete removal of DMF from the channels of **1**. It is also notable that the decomposition temperature of 417 °C is substantially higher than for the Mn, Fe, or Co formate analogues, which all decompose at approximately 270 °C.[10a,10d,12a] These findings are consistent with the thermal decomposition of magnesium formate dihydrate, which is reported to take place in three stages, with a final decomposition at approximately 452 °C.[24] Presumably, the increased ionic nature of the bonding in the magnesium formate leads to a substantially higher thermal stability compared to that of the transition-metal analogues.

Powder XRD analysis was used in order to determine whether the crystallinity of the bulk material remained intact after guest removal. A crystalline sample of **1** was evacuated under a dynamic vacuum at 130 °C for 36 h, and the resulting crystals were then used for subsequent studies. Figure 4 shows both the experimental and calculated powder XRD patterns for the evacuated compound $[Mg_3(O_2CH)_6]$, **2**, which are in excellent agreement. Complete guest removal was also confirmed by IR and NMR spectroscopic analyses. For the ^{1}H NMR studies, the evacuated crystals were solubilized in D_2O, and the spectra of the resulting solution indicated only the presence of the formate.

Single-crystal XRD analysis was also successfully completed on the evacuated material. Crystallographic details for **2** can be found in Table 1. As shown in Figure 2b, the framework is retained upon evacuation, with only relatively minor changes to the structure. To illustrate, the independent Mg−O distances and O−Mg−O angles vary by less than 0.02 Å and 4.2°, respectively, between **1** and **2**. The unit cell volumes are also similar, at 1640 Å^3 for **1** and 1630 Å^3 for **2**.

Both N_2 and H_2 gas sorption experiments were carried out on **1** at 77.4 K, and the isotherms obtained are shown in Figures 5 and 6. Both plots indicate limited hysteresis. The framework showed an N_2 uptake of approximately 88 mL/g, with a BET surface area of 150 m^2/g. Micropore analysis using the *t*-plot method determined the pore volume to be 0.043 mL/g and the pore area to be 104 m^2/g. Also, H_2 sorption studies on **1** indicated an uptake of 70 mL/g, which corresponds to 0.6 wt %. These studies therefore confirm that the evacuated framework exhibits permanent porosity. In comparison, studies by Kim indicate that the manganese framework β-$[Mn_3(O_2CH)_6]$ does not display sorption of N_2, CH_4, or Ar but does uptake CO_2 and H_2 to give BET surfaces areas of 297 m^2/g and 240 m^2/g, respectively.[11] The H_2 sorption in this case is approximately 100 mL/g, or 0.9 wt %. Although these H_2 sorptions are somewhat moderate, they compare well with the value of 0.7 wt % obtained for the highest capacity zeolite ZSM-5. In independent studies, Wang confirmed the inability of the manganese framework to uptake N_2 but was able to demonstrate that the cobalt derivative $[Co_3(O_2CH)_6]$ displays a N_2 sorption of 108 mL/g, with a BET surface area of 360 m^2/g and a pore volume of 0.15 mL/g.[10d]

Next, we were interested in the possibility of using the evacuated framework **2** to uptake small molecules from solution. Wang previously delineated in a preliminary communication that β-$[Mn_3(O_2CH)_6]$ can uptake a large variety of guest molecules from solution, but only limited structural details were outlined.[10a,c] Crystals of **2** were soaked for 2 days in eight different solvent systems: DMF, THF, Et_2O, acetone, benzene, ethanol, methanol, and cyclohexane. Afterward, they were filtered and dried in air. Crystals from each system were then dissolved in D_2O and analyzed by ^{1}H NMR spectroscopy. With the exception of cyclohexane, the spectra showed the presence of both formate and guest, indicating solvent uptake. This was then confirmed by single-crystal XRD studies, which characterized the formation of the new inclusion materials $[Mg_3(O_2CH)_6\supset THF]$, **3**; $[Mg_3(O_2CH)_6\supset Et_2O]$, **4**; $[Mg_3(O_2CH)_6\supset Me_2CO]$, **5**; $[Mg_3(O_2CH)_6\supset C_6H_6]$, **6**; $[Mg_3(O_2CH)_6\supset EtOH]$, **7**; and $[Mg_3(O_2CH)_6\supset MeOH]$, **8**. Crystallographic details of these compounds are given in Table 1 (full lists of Mg−O bond lengths and O−Mg−O angles are available in the Supporting Information). As expected, the complexes are isomorphous and contain one guest molecule per asymmetric unit. The network may also be described as an extended diamondoid lattice, with the metals acting as tetrahedral nodes spaced apart by linear-linking metal nodes. This description leads to the observation that a single guest molecule resides within each of the pseudo-adamantane cavities (Figure 7) and that the channels are formed down the *b* axis by fusion of the

(28) Allen, F. H.; Kennard, O.; Watson, D. G.; Brammer, L.; Orpen, A. G. *J. Chem. Soc., Perkin Trans.* **1987**, S1.
(29) Spek, A. L. *PLATON, A Multipurpose Crystallographic Tool*; Utrecht University: Utrecht, The Netherlands, 2001.
(30) Watanabe, T.; Matsui, M. *Acta Crystallogr., Sect. B* **1980**, *36*, 1081.
(31) Watanabe, T.; Matsui, M. *Acta Crystallogr., Sect. B* **1978**, *34*, 2731.

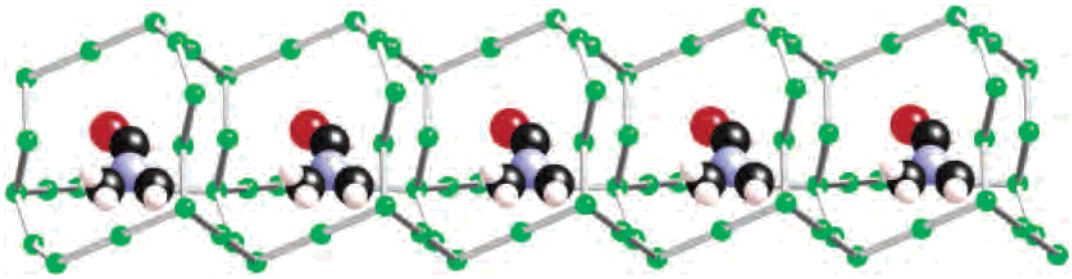

Figure 7. Section of **1** showing the guest DMF molecules within a series of fused adamantane cavities. The green spheres represent the tetrahedral and linear metal nodes of the extended diamondoid framework.

adamantane units. With the exceptions of ethanol and methanol, all of the guest molecules were found to be well-behaved on refinement of the structures with no significant disorder problems. The ethanol and methanol complexes **7** and **8** were refined with two-and three-site disorder, respectively. The approximate volumes of the guest molecules range from 41 Å^3 for methanol to 100 Å^3 for benzene.[33] Cyclohexane has an approximate volume of 112 Å^3 and presumably did not diffuse into the channels because of size exclusion.

^{1}H NMR spectroscopic studies in D_2O also proved to be valuable for investigating the selectivity of **2** using mixtures of solvents.[34] A series of experiments were undertaken by soaking crystals of **2** in 1:1 bicomponent volumetric mixtures of the six solvents DMF, THF, acetone, benzene, ethanol, and methanol. Although each system was found to uptake guests, only the experiments involving mixtures with benzene were found to show any significant selectivity. In these instances, only trace amounts of benzene could be detected, again presumably due to this being the largest of the molecules studied. Similarly, mixing equal volumes of all six of these solvents in a single vial followed by soaking crystals of **2** resulted in uptake of each of these guests but with only trace amounts of benzene.

Finally, the effect of the occluded guest on the frameworks of **1**−**8** can be gauged by comparison of the eight crystal structures. Overall, the frameworks are very similar, with the individual Mg−O distances and the O−Mg−O angles varying by less than 0.034 Å and 4.3°, respectively. Summarized analyses are given in Tables 2 and 3. The unit cell volumes vary from 1612 Å^3 for **8** (MeOH inclusion) to 1707 Å^3 for **6** (benzene inclusion), i.e., an increase of approximately 5.9% between **8** and **6**. However, excluding the benzene complex **6**, the unit cell volumes of the other seven materials vary only between 1612 and 1641 Å^3, with the guest-free compound **2** having an intermediate cell volume of 1630 Å^3. These cell-volume changes illustrate flexibility where the framework may contract to maximize the attractive interactions with the guests or, alternatively, expand to allow inclusion of larger guest molecules.

Conclusions

We have demonstrated that the α-form of unsolvated magnesium formate may be prepared in a high-quality crystalline form at elevated temperature using DMF as solvent media. The resulting framework is both thermally robust (substantially more so than the transition-metal analogues) and also remains intact after guest removal. Gas sorption studies indicate that the material is porous and can uptake both N_2 and H_2, albeit in only very moderate amounts in comparison to other MOFs.[9,35] The guest-exchange studies show that a range of small molecules may be incorporated into the framework and that selective separations are possible by size exclusion. On the basis of the present work, further studies are underway to investigate the possibility of preparing metal complexes of derivatized small carboxylates to produce functionalized, porous, and lightweight framework materials.

Acknowledgment. We gratefully acknowledge the Petroleum Research Fund (41716-AC3) and the National Science Foundation (CHE-0443233) for instrumentation support. Also, thanks to Professor Paul McGinn and Hongmei An (University of Notre Dame) for help with the TGA studies, and Donald Weirick at Ouantachrome Instruments for aid with the gas sorption studies.

Supporting Information Available: Crystallographic data for compounds **1**−**8** and **13**−**15** in CIF format as well as tables of bond lengths and angles. This material is available free of charge via the Internet at http://pubs.acs.org.

IC060543V

(32) Mentzen, B. F.; Comell, C. *J. Solid State Chem.* **1974**, *9*, 214.
(33) Molecular volumes were calculated using the *Spartan 04* program, Wavefunction Inc., Irvine, CA. Each guest molecule was geometry optimized using the semiempirical AM1 method.
(34) Horner, M. J.; Grbowski, S.; Sandstrom, K.; Holma, K. T.; Bader, M.; Ward, M. *Trans. Am. Crystallogr. Assoc.* **2004**, *39*, 130.
(35) Navarro, J. A. R.; Barea, E.; Salas, J. M.; Masciocchi, N.; Galli, S.; Sironi, A.; Ania, C. O.; Parra, J. O. *Inorg. Chem.* **2006**, *45*, 2397.